Temperature-Dependent Bending Rigidity of *AB*-Stacked Bilayer Graphene

S. D. Eder,[1] S. K. Hellner,[1] S. Forti,[2] J. M. Nordbotten,[3] J. R. Manson,[4,5] C. Coletti,[2] and B. Holst[1]
[1]Department of Physics and Technology, University of Bergen, Allégaten 55, 5007 Bergen, Norway
[2]Center for Nanotechnology Innovation@NEST, Istituto Italiano di Tecnologia, Piazza San Silvestro 12, 56127 Pisa, Italy
[3]Department of Mathematics, University of Bergen, Allégaten 41, 5007 Bergen, Norway
[4]Department of Physics and Astronomy, Clemson University, Clemson, South Carolina 29634, USA
[5]Donostia International Physics Center (DIPC), Paseo Manuel de Lardizabal, 4, 20018 Donostia-San Sebastián, Spain

(Received 20 May 2021; accepted 28 October 2021; published 23 December 2021)

The change in bending rigidity with temperature $\kappa(T)$ for 2D materials is highly debated: theoretical works predict both increase and decrease. Here we present measurements of $\kappa(T)$, for a 2D material: *AB*-stacked bilayer graphene. We obtain $\kappa(T)$ from phonon dispersion curves measured with helium atom scattering in the temperature range 320–400 K. We find that the bending rigidity increases with temperature. Assuming a linear dependence over the measured temperature region we obtain $\kappa(T) = [(1.3 \pm 0.1) + (0.006 \pm 0.001)T/K]$ eV by fitting the data. We discuss this result in the context of existing predictions and room temperature measurements.

DOI: 10.1103/PhysRevLett.127.266102

Mechanical properties of 2D materials are important for fundamental understanding and for a range of application areas, for example, flexible electronics. To design electronic components that do not fracture when bent, it is important to know how flexible the different material layers are relative to each other and how this flexibility changes with temperature. This is expressed by the bending rigidity κ sometimes referred to as bending stiffness or flexural rigidity: a measure of material resistance to deformation. In classical mechanics κ can be derived for an isotropic plate with thickness h, Young's modulus Y, and Poisson's ratio σ as [1]

$$\kappa(h) = \frac{Yh^3}{12(1-\sigma)}. \tag{1}$$

The unit of κ is $[\mathrm{Pa} \times \mathrm{m}^3] = [\mathrm{J}]$, usually expressed in [eV] for nanomaterials. For crystalline materials, the elastic properties are described by a tensor. However, for hexagonal crystals such as graphite the elastic properties in the (0001) plane can be treated as isotropic [1]. A relatively simple method for measuring Y and σ for 2D materials is to use an atomic force microscope to poke with a well-defined force and measure the response (nanoindentation) [2]. It should then be possible to determine κ from the formula above. However, this implies knowing the thickness h, which is difficult to determine for 2D materials, as reflected in the "Yakobson's paradox" debate in the graphene community a few years back, see, for example, Refs. [3–5]. Furthermore, the formula implies that the 2D materials behave classically, which is not necessarily the case.

Numerous experiments have investigated mechanical properties of 2D materials using various forms of nanoengineering. For a review, see Ref. [2]. However, the bending rigidity has proven difficult to measure due to contributions from extrinsic stiffening from out of plane corrugations or in-plane strain. The reported values (experiment and theory) range from around 0.85 to 10 eV for monolayer graphene [6–14] and 3 to 180 eV for bilayer graphene [9,13,15–19]. A recent experimental paper claims that the bending rigidity at room temperature for few-layer graphene decreases with bending angle [17].

A few years ago, a theoretical paper showed how the bending rigidity for an isotropic, free-standing thin membrane can be obtained from a phonon dispersion curve where the membrane is weakly bound to a substrate as [20]

$$\omega(\Delta K) = \sqrt{\frac{\kappa}{\rho_{2\mathrm{D}}}\Delta K^4 + {\omega_0}^2}, \tag{2}$$

where ω is the phonon frequency, ΔK the parallel component of the wave-vector transfer, $\rho_{2\mathrm{D}}$ is the density of the 2D material and ω_0 the binding energy between the thin membrane and the substrate. Note that as long as the sample is only weakly bound to the substrate, it is the free-standing 2D material value for κ that is measured. Strictly speaking, for an infinite extent thin film with fixed or periodic boundary conditions, Eq. (2) should also contain a quadratic term in ΔK within the argument of the square root, implying the weak linear term in the dispersion relation. However, this term is typically small compared to the binding energy and is therefore usually ignored [21].

In 2015 Al Taleb *et al.* applied this theory for the first time to measure the bending rigidity of free-standing monolayer graphene [12] using phonon dispersion curves from monolayer graphene on copper obtained with helium

scattering. For recent reviews of helium scattering see Refs. [22,23]. Al Taleb *et al.* obtained the first experimental measurement of κ for monolayer graphene, which shows good agreement with theory. Experimental results for graphene previous to this publication gave much higher values due to challenges with out-of-plane corrugations and strain as discussed above [2]. The experimental value often cited in the literature which agrees well with theory actually stems from Raman spectroscopy on bulk graphite [24]. To the best of our knowledge, the Al Taleb work remains the most precise measurement of the bending rigidity of monolayer graphene ever obtained. The bending rigidity of monolayer graphene has since been measured with helium scattering on other weakly bound substrates such as sapphire, demonstrating how deviation in bending rigidity can be used to quantify defects [25]. In 2018 some of the present authors and co-workers measured the bending rigidity of bilayer silica using the same method as Al Taleb *et al.* The result agrees well with theoretical predictions [26].

Up until now no experimental Letter has addressed the issue of temperature dependence of the bending rigidity $\kappa(T)$ of 2D materials, even though it is highly debated in the literature. For graphene both a decrease [27,28] as well as an increase [10,29,30] of the bending rigidity with temperature has been predicted. For bilayer graphene, there are also conflicting results. Zero-temperature *ab initio* calculations predict $\kappa = 162.7$ [19] and 180 eV [16] whereas experimental work at room temperature yields values of around 3–35 eV [8,9,15,17]. Taken together these results suggest a decrease in the bending rigidity with temperature. In contrast, a theoretical paper calculates the temperature dependence of the bending rigidity of bilayer graphene predicting it to increase with temperature [18] and pointing out with reference to Ref. [31] that an increase in bending rigidity with temperature is generally to be expected for crystalline membranes. Reference [18] also predicts that the bending rigidity of bilayer graphene is twice that of monolayer graphene for all temperatures, rather than a factor 8 as would be expected from the classical formula, assuming the thickness of bilayer graphene to be twice that of monolayer graphene, see Eq. (1). As mentioned in the introduction the thickness of monolayer graphene has been a topic of debate, with different plausible approaches yielding very different values (the Yakobson paradox) [3–5]. We note that for the method presented by Al Taleb *et al.* only knowledge about the 2D material density is required to obtain the bending rigidity [12]. In the most recent theoretical paper on temperature dependence of bending rigidity of graphene that we found, the authors, while not presenting any numbers, state that they expect the bending rigidity of bilayer graphene to also increase with temperature [29].

Here we present measurements of the variation of bending rigidity with temperature for a 2D material. We performed our measurements on a bilayer graphene sample on H-terminated SiC(0001) prepared at the Istituto Italiano di Tecnologia (IIT) on a N-doped ($10^{18}/\mathrm{cm}^3$) 6H-SiC(0001) crystal from Crystal GmbH. The sample was prepared using an established procedure at the institute: First the substrate was etched in a 50% Ar and H_2 mixture with a total pressure of 450 mbar (fluxes 500 sccm each) at 1200 °C for 5 min to regularize the step-terrace morphology. Then, following the method introduced by Emtsev *et al.* [32], a graphene monolayer was obtained on top of the C-rich reconstruction $(6\sqrt{3} \times 6\sqrt{3})R30°$ of the SiC(0001) plane [33,34], by heating the sample in a 750 mbar Ar atmosphere at 1310 °C for 4 min. Finally the sample was exposed to a 50% Ar and H_2 mixture with a total pressure of 750 mbar (fluxes 500 sccm each) at 800 °C for 20 min. This leads to atomic hydrogen intercalating at the hetero-interface between SiC(0001) and the carbon rich surface reconstruction, thereby lifting the covalent interaction so that the carbon atoms previously in the reconstruction form a monolayer of graphene on top of the now H-terminated SiC(0001) [35–37]. The resulting bilayer is predominantly *AB*, though small deviations from the ideal *AB* stacking can occur [38]. The sample quality (structure and coverage) was assessed at IIT using Raman spectroscopy, scanning tunneling microscopy (STM), atomic force microscopy (AFM), and low energy electron diffraction (LEED). See Figs. S4–S6 and discussion in the Supplemental Material [39].

Bilayer graphene on H-terminated SiC(0001) is referred to in the literature as quasi-free-standing bilayer graphene [35] and as the name says is weakly bound to the substrate because of the hydrogen intercalation which lifts the covalent bond. In fact it can be peeled off the substrate in a manner similar to graphene on Cu [47]. Because the sample is weakly bound to the substrate we can use the phonon dispersion curve model, Eq. (2), described above to obtain the bending rigidity for the free-standing bilayer. A particular advantage of using this model is that the temperature of the 2D material can be easily and uniformly varied by changing the temperature of the underlying SiC(0001) substrate.

After preparation, the sample was removed from the preparation chamber and placed in a sealed package, filled with ambient air from the laboratory (humidity 50%, temperature 22°C) and shipped to the University of Bergen (UiB). The sealed package was stored in the laboratory for a few days before the sample was mounted in the argon vented sample chamber of the molecular beam apparatus known as MAGIE at UiB, which was then pumped down. The neutral helium beam was created by a supersonic (free-jet) expansion from a source reservoir through a (10 ± 0.5) μm diameter nozzle [48]. The central part of the beam was selected by a skimmer, (410 ± 2) μm in diameter, placed (11.6 ± 0.5) mm in front of the nozzle. The sample was characterized in vacuum, by helium

diffraction scans and time of flight (TOF) spectra using a pseudorandom chopper [49]. The background pressure during all measurements was around 1×10^{-9} mbar or less. The incident beam spot size on the sample was around 4 mm in diameter for all measurements. A diffraction pattern could be obtained immediately after installing the sample and pumping down, without any preparation, but a bake-out for 1 h at $T_s = 675$ K improved the signal, yielding a high intensity specular peak, with a measured full width at half maximum of (0.0254 ± 0.004) Å^{-1}, corresponding to the instrument resolution limit, see Figs. S2 and S3 in the Supplemental Material [39]. The bake-out procedure was repeated in between measurements..

Figure 1 shows phonon dispersion curves obtained at three different temperatures using helium atom scattering. The solid curves show best fits obtained using the model presented in Eq. (2). The overall shape of the measured dispersion curve is in excellent agreement with the model. We use these fits to obtain the bending rigidity as a function of temperature (Fig. 2) using the measured density of our bilayer graphene sample, $\rho_{2D} = 1.56 \times 10^{-6}$ kg/m^2 (see the Supplemental Material [39]). This value is very close to the theoretically expected value for bilayer graphene: $\rho_{2D} = 1.52 \times 10^{-6}$ kg/m^2. We see that the bending rigidity increases with temperature, a linear, weighted fit gives

$$\kappa(T) = [(1.3 \pm 0.1) + (0.006 \pm 0.001)T/\mathrm{K}]\ \mathrm{eV}. \quad (3)$$

The errors are the standard errors from the weighted fit. We note that the linear fit is to be taken with caution. It is a good fit in the relatively small temperature range that we investigate. It is not necessarily to be expected that the behavior is linear over a larger range [18].

In Fig. 2 we also include room temperature bending rigidity measurements from two of the three experimental publications on the bending rigidity of bilayer graphene [15,17]. The measurements were done by either measuring the curvature of folded exfoliated sheets [15] (large bending angle) or by measuring the curvature of exfoliated sheets draped over step edges of varying heights [17] (varying bending angle between around 4° and 80°). We did not include the measurement published in Ref. [9] (the earliest of the three publications) because it is an order of magnitude larger. We attribute this to strain induced during the fabrication process. We note the rather puzzling fact that our measurements agree very well with the large bending angle results in Ref. [17] and in Ref. [15] but less so with the small bending angle result in Ref. [17]. We also plot the theoretically predicted curve from Ref. [18] as a black dashed line in Fig. 2. Most importantly, our measurements

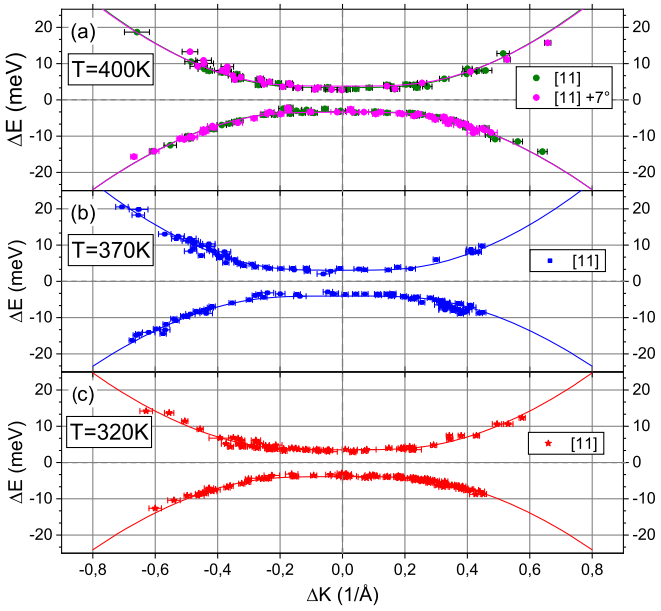

FIG. 1. Phonon dispersion curves of bilayer graphene on SiC(0001), obtained for different sample temperatures T using helium atom time of flight scattering. All measurements are done along the [11] axis, except one measurement where the crystal was rotated in the plane 7°° away from the [11] axis, to verify that the elastic properties are isotropic in the plane. The lines present fits according to Eq. (2) with $\Delta E = \hbar\omega$. For each T the lower curve with negative energies corresponds to helium atom energy loss (phonon creation), the upper curve with positive energies corresponds to helium atom energy gain (phonon annihilation). The error bars for ΔE are smaller than the data points. A description of the error bar evaluation can be found in the last section of the Supplemental Material [39].

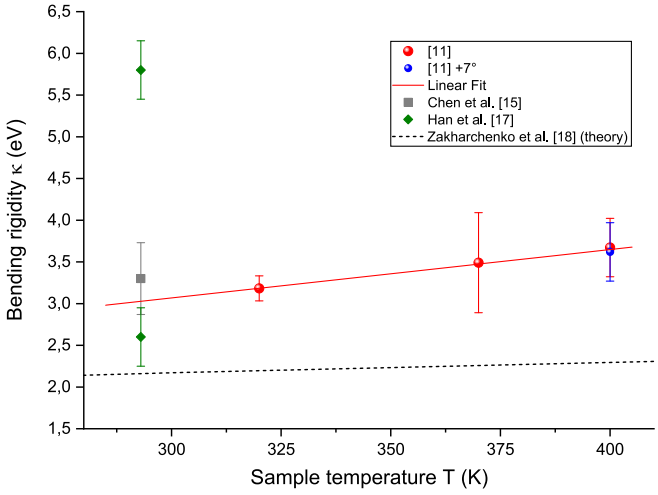

FIG. 2. Bending rigidity values obtained from dispersion curve fits (see Fig. 1) and plotted as a function of temperature with a linear fit (red line).The dashed black line is a theoretical prediction taken from Ref. [18]. We also show three data points from previous room temperature experiments (not included in our fit). The top point (green diamond [17]) is obtained from small angle bending, the two lower points (green diamond [17] and gray square [15]) are obtained for high angle bending. A description of the error bar evaluation can be found in the last section of the Supplemental Material [39].

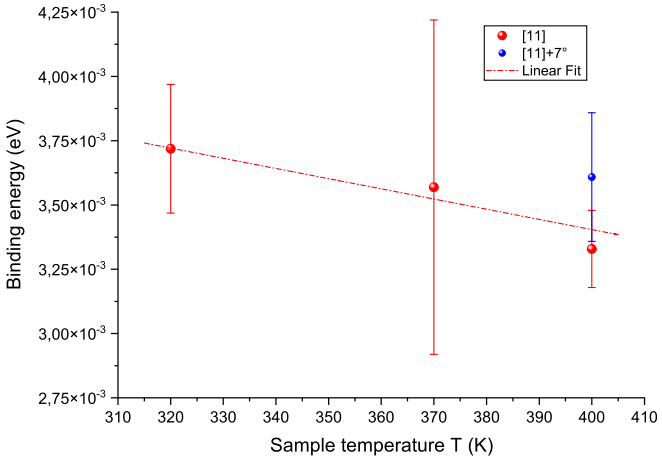

FIG. 3. Temperature dependence of the binding energy $\hbar\omega_0$ between the bilayer and the substrate. The error bars were determined in a similar manner as in Fig. 2; see explanation at the end of the Supplemental Material [39].

clearly show that the bending rigidity increases with temperature as predicted in Ref. [18]. The theoretically predicted slope in this temperature range is around 0.001 eV/K, which is lower than the slope we measure [see Eq. (3)]. Furthermore, the theoretically predicted values all lie below the experimental values measured by us and others. We note that the predictions for the bending rigidity of graphene, presented in Ref. [18] are also lower than what has been experimentally measured. Finally, Ref. [18] presents the general prediction that the bending rigidity of bilayer graphene should be twice that of the bending rigidity of graphene. Within error bars we measure twice the value measured by Al Taleb *et al.* for graphene on copper [12] and also twice the value measured on graphene flakes as recently presented [17]. In a recent paper [30] the temperature-dependent bending rigidity of single-layer graphene is modeled using modal analysis. In the temperature range 300–400 K the dependence was approximated well with a linear fit with a slope of 0.003 eV/K—exactly half the value that we measure for bilayer graphene. Noting the prediction that the bending rigidity of bilayer graphene should be exactly twice that of single-layer graphene, this is excellent agreement.

Finally, we use the fits of the data from from Fig. 1 to Eq. (2) in order to determine the binding energy $\hbar\omega_0$ between the bilayer graphene and the SiC(0001) substrate. The binding energies for different temperatures are shown in Fig. 3. As one would expect, there is indication of a weak decrease of the binding energy with temperature. The values that we measure are comparable to what has been measured previously for other very weakly bound 2D materials: graphene on copper [12] and sapphire [25] and bilayer silica on ruthenium [26].

To conclude, we have performed measurements of the variation of the bending rigidity with temperature for a 2D material: *AB*-stacked bilayer graphene. We show that the bending rigidity increases with temperature in agreement with theoretical calculations for bilayer graphene and the general theory of crystalline membranes. Our results also agree well with recent experiments made only at room temperature. The next step will be to perform further measurements covering larger temperature ranges and on other 2D materials such as single-layer graphene and bilayer silica glass [26]. Of further interest would be to investigate layered structures of van der Waals materials whose bending rigidity has been measured by other methods [50]. Other layered materials of interest include the pnictogen chalcogenides of which several have already had some surface properties measured by He atom scattering [51,52].

[1] L. D. Landau, L. P. Pitaevskii, A. M. Kosevich, and E. M. Lifshitz, *Theory of Elasticity* (Butterworth, Heinemann, London, 2012).
[2] D. Akinwande, C. J. Brennan, J. Scott Bunch, P. Egberts, J. R. Felts, H. Gao, R. Huang, J. Kim, T. Li, Y. Li, K. M. Liechti, N. Lu, H. S. Park, E. J. Reed, P. Wang, B. I. Yakobson, T. Zhang, Y.-W. Zhang, Y. Zhou, and Y. Zhu, A review on mechanics and mechanical properties of 2d materials—graphene and beyond, Extreme Mech. Lett. **13**, 42 (2017).
[3] L. Wang, Q. Zheng, J. Z. Liu, and Q. Jiang, Size Dependence of the Thin-Shell Model for Carbon Nanotubes, Phys. Rev. Lett. **95**, 105501 (2005).
[4] P. Pine, Y. Yaish, and J. Adler, Vibrational analysis of thermal oscillations of single-walled carbon nanotubes under axial strain, Phys. Rev. B **89**, 115405 (2014).
[5] Y. Huang, J. Wu, and K. C. Hwang, Thickness of graphene and single-wall carbon nanotubes, Phys. Rev. B **74**, 245413 (2006).
[6] J. Zhao, Q. Deng, T. H. Ly, G. H. Han, G. Sandeep, and M. H. Rümmeli, Two-dimensional membrane as elastic shell with proof on the folds revealed by three-dimensional atomic mapping, Nat. Commun. **6**, 8935 (2015).
[7] M. K. Blees, A. W. Barnard, P. A. Rose, S. P. Roberts, K. L. McGill, P. Y. Huang, A. R. Ruyack, J. W. Kevek, B. Kobrin, D. A. Muller, and P. L. McEuen, Graphene kirigami, Nature (London) **524**, 204 (2015).
[8] Y. K. Shen and H. A. Wu, Interlayer shear effect on multilayer graphene subjected to bending, Appl. Phys. Lett. **100**, 101909 (2012).
[9] N. Lindahl, D. Midtvedt, J. Svensson, O. A. Nerushev, N. Lindvall, A. Isacsson, and E. E. B. Campbell, Determination of the bending rigidity of graphene via electrostatic actuation of buckled membranes, Nano Lett. **12**, 3526 (2012).
[10] K. V. Zakharchenko, M. I. Katsnelson, and A. Fasolino, Finite Temperature Lattice Properties of Graphene beyond the Quasiharmonic Approximation, Phys. Rev. Lett. **102**, 046808 (2009).
[11] E. Ertekin, D. C. Chrzan, and M. S. Daw, Topological description of the stone-wales defect formation energy in carbon nanotubes and graphene, Phys. Rev. B **79**, 155421 (2009).

[12] A. Al Taleb, H. K. Yu, G Anemone, D. Farias, and A. M. Wodtke, Helium diffraction and acoustic phonons of graphene grown on copper foil, Carbon **95**, 731 (2015).
[13] Y. Guo, J. Qiu, and W. Guo, Mechanical and electronic coupling in few-layer graphene and hbn wrinkles: A first-principles study, Nanotechnology **27**, 505702 (2016).
[14] Y. Wei, B. Wang, J. Wu, R. Yang, and M. I. Dunn, Bending rigidity and gaussian bending stiffness of single-layered graphene, Nano Lett. **13**, 26 (2013).
[15] X. Chen, C. Yi, and C. Ke, Bending stiffness and interlayer shear modulus of few-layer graphene, Appl. Phys. Lett. **106**, 101907 (2015).
[16] P. Koskinen and O. O. Kit, Approximate modelling of spherical membranes, Phys. Rev. B **82**, 235420 (2010).
[17] E. Han, Y. Jaehyung, E. Annevelink, J. Son, D. A. Kang, K. Watanabe, T. Taniguchi, E. Ertekin, P. U. Huang, and A. M. van der Zande, Ultrasoft slip-mediated bending in few-layer graphene, Nat. Mater. **19**, 305 (2020).
[18] K. V. Zakharchenko, J. H. Los, M. I. Katsnelson, and A. Fasolino, Atomistic simulations of structural and thermodynamic properties of bilayer graphene, Phys. Rev. B **81**, 235439 (2010).
[19] D. B. Zhang, E. Akatyeva, and T. Dumitrica, Bending Ultrathin Graphene at the Margins of Continuum Mechanics, Phys. Rev. Lett. **106**, 255503 (2011).
[20] B. Amorim and F. Guinea, Flexural mode of graphene on a substrate, Phys. Rev. B **88**, 115418 (2013).
[21] G. Benedek, J. R. Manson, and S. Miret-Artès, The electron-phonon coupling constant for single-layer graphene on metal substrates determind from he atom scattering, Phys. Chem. Chem. Phys. **23**, 7575 (2021).
[22] B. Holst and G. Bracco, Probing surfaces with thermal He atoms: Scattering and microscopy with a soft touch, in *Surface Science Techniques*, book section 12 (Springer Verlag, Berlin, 2013).
[23] B. Holst, G. Alexandrowicz, N. Avidor, G. Benedek, G. Bracco, W. E. Ernst, D. Farias, A. P. Jardine, K. Lefmann, J. R. Manson, R. Marquardt, S. Miret-Artès, S. J Sibener, J. W. Wells, A. Tamtögl, and W. Allison, Material properties particularly suited to be measured with helium scattering: Selected examples from 2D materials, van der Waals heterostructures, glassy materials, catalytic substrates, topological insulators and superconducting radio frequency materials, Phys. Chem. Chem. Phys. **23**, 7653 (2021).
[24] R. Nicklow, N. Wakabayashi, and H. G. Smith, Lattice dynamics of pyrolytic graphite, Phys. Rev. B **5**, 4951 (1972).
[25] G. Anemone, E. Climent-Pascual, H. K. Yu, A. Al Taleb, F. Jimenez-Villacorta, C. Prieto, A. M. Wodtke, A. D. Andres, and D. Farias, Quality of graphene on sapphire: Long-range order from helium diffraction versus lattice defects from raman spectroscopy, RSC Adv. **6**, 21235 (2016).
[26] C. Büchner, S. D. Eder, T. Nesse, D. Kuhness, P. Schlexer, G. Pacchioni, J. R. Manson, M. Heyde, B. Holst, and H.-J. Freund, Bending Rigidity of 2D Silica, Phys. Rev. Lett. **120**, 226101 (2018).
[27] P. Liu and Y. W. Zhang, Temperature-dependent bending rigidity of graphene, Appl. Phys. Lett. **94**, 231912 (2009).
[28] L. Shen, H.-S. Shen, and C.-L. Zhang, Temperature-dependent elastic properties of single layer graphene sheets, Mater. Des. **31**, 4445 (2010).
[29] Y. Lijun, Temperature dependence bending rigidity of 2d membranes: Graphene as an example, AIP Adv. **8**, 075104 (2018).
[30] B. Sajadi, S. van Hemert, B. Arash, P. Berlardinelli, P. G. Steeneken, and F Alijani, Size- and temperature-dependent bending rigidity of graphene using modal analysis, Carbon **139**, 334 (2018).
[31] D. R. Nelson and L. Peliti, Fluctuations in membranes with crystalline and hexatic order, J. Phys. (Les Ulis, Fr.) **48**, 1085 (1987).
[32] K. V. Emtsev, A. Bostwick, K. Horn, J. Jobst, G. L. Kellog, L. Ley, J. L. McChesney, T. Ohta, S. A. Reshanov, J. Röhrl, E. Rotenberg, A. K. Schmid, D. Waldmann, H. B. Weber, and T. Seyller, Towards wafer-size graphene layers by atmospheric pressure graphitization of silicon carbide, Nat. Mater. **8**, 203 (2009).
[33] K. V. Emtsev, F. Speck, Th. Seyller, L. Ley, and J. D. Riley, Interaction, growth and ordering of epitaxial graphene on SiC0001 surfaces: A comparative photoelectron spectroscopy study, Phys. Rev. B **77**, 155303 (2008).
[34] S. Forti and U. Starke, Epitaxial graphene on SiC: From carrier density engineering to quasi-free standing graphene by atomic intercalation, J. Phys. D **47**, 094013 (2014).
[35] C. Riedl, C. Coletti, T. Iwasaki, A. A. Zakharov, and U. Starke, Quasi-Free-Standing Epitaxial Graphene on SiC Obtained by Hydrogen Intercalation, Phys. Rev. Lett. **103**, 246804 (2009).
[36] S. Forti, K. V. Emtsev, C. Coletti, A. A. Zakharov, C. Riedl, and U. Starke, Large-area homogeneous quasifree standing epitaxial graphene on SiC(0001): Electronic and structural characterization, Phys. Rev. B **84**, 125449 (2011).
[37] S. Forti, *Growing Graphene on Semiconductors* (Pan Stanford Publishing, Singapore, 2017), pp. 141–80.
[38] K. S. Kim, A. L. Walter, L. Moreshini, T. Seyller, K. Horn, E. Rotenberg, and A. Bostwick, Coexisting massive and massless Dirac fermions in symmetry-broken bilayer graphene, Nat. Mater. **12**, 887 (2013).
[39] See Supplemental Material at http://link.aps.org/supplemental/10.1103/PhysRevLett.127.266102 for sample characterization, which includes Refs. [40–46].
[40] S. Forti and U. Starke, Epitaxial graphene on SiC: From carrier density engineering to quasi-free standing graphene by atomic intercalation, J. Phys. D **47**, 094013 (2014).
[41] S. Forti, K. V. Emtsev, C. Coletti, A. A. Zakharov, C. Riedl, and U. Starke, Large-area homogeneous quasifree standing epitaxial graphene on SiC(0001): Electronic and structural characterization, Phys. Rev. B **84**, 125449 (2011).
[42] A. C. Ferrari and D. M. Basko, Raman Spectroscopy as a versatile tool for studying the properties of graphene. Nat. Nanotechnol. **8**, 235 (2013).
[43] L. M. Malard, J. Nilsson, D. C. Elias, J. C. Brant, F. Plentz, E. S. Alves, A. H. Castro Neto, and M. A. Pimenta, Probing the electronic structure of bilayer graphene by Raman scattering, Phys. Rev. B **76**, 201401(R) (2007).
[44] M. Yankowitz, J. I. J. Wang, S. Li, A. G. Birdwell, Y. A. Chen, K. Watanabe, T. Taniguchi, A. Y. Quek, P. Jarillo-Herrero, and B. J. LeRoy, Band structure mapping of bilayer graphene via quasiparticle scattering, APL Mater. **2**, 092503 (2014).

[45] M. Bayle, N. Reckinger, J. R. Huntzinger, A. Felten, A. Bakaraki, P. Landois, J. F. Colomer, L. Henrard, A. A. Zahab, J. L. Sauvajol, and M. Paillet, Dependence of the Raman spectrum characteristics on the number of layers and stacking orientation in few-layer graphene, Phys. Status Solidi B **252**, 2375 (2015).

[46] U. Starke, Ch. Bram, P.-R. Steiner, W. Hartner, L. Hammer, K. Heinz, and K. Müller, The (0001)-surface of 6H-SiC: morphology, composition and structure, Appl. Surf. Sci. **89**, 175 (1995).

[47] K. Liu, P. Yan, J. Li, C. He, T. Ouyang, C. Zhang, C. Tang, and J. Zhong, Effect of hydrogen passivation on the decoupling of graphene on SiC(0001) substrate: First-principles calculations, Sci. Rep. **7**, 8461 (2017).

[48] S. D. Eder, B. Samelin, G. Bracco, K. Ansperger, and B. Holst, A free jet (supersonic), molecular beam source with automatized, 50 nm precision nozzle-skimmer positioning, Rev. Sci. Instrum. **84**, 093303 (2013).

[49] D. D. Koleske and S. J. Sibener, Generation of pseudorandom sequences for use in cross-corelation modulation, Rev. Sci. Instrum. **63**, 3852 (1992).

[50] G. Wang, Z. Dai, J. Xio, S. Feng, C. Weng, L. Liu, Z. Xu, R. Huang, and Z. Zhang, Bending of Multilayer van der Waals Materials. Phys. Rev. Lett. **123**, 116101 (2014).

[51] A. Tamtögl, D. Campi, M. Bremholm, E. M. J. Hedegaard, B. B. Iversen, M. Bianchi, P. Hofmann, N. Marzari, G. Benedek, J. Ellis, and W. Allison, Nanoscale surface dynamics of $Bi_2Te_3(111)$: Observation of a prominent surface acoustic wave and the role of van der Waals interactions, Nanoscale **10**, 14627 (2018).

[52] A. Ruckhofer, D. Campi, M. Bremholm, P. Hofmann, G. Benedek, M. Bernasconi, W. E. Ernst, and A. Tamtögl, Terahertz surface modes and electron-phonon coupling on $Bi_2Se_3(111)$, Phys. Rev. Research **2**, 023186 (2020).